

Article

Synergistic Effect of Alkali Na and K Promoter on Fe-Co-Cu-Al Catalysts for CO₂ Hydrogenation to Light Hydrocarbons

Yuhao Zheng, Chenghua Xu *, Xia Zhang, Qiong Wu and Jie Liu

College of Resources and Environment, Chengdu University of Information Technology, Chengdu 610225, China; daimi4126@cuit.edu.cn (Y.Z.); yl@cuit.edu.cn (X.Z.); flower@cuit.edu.cn (Q.W.); ljzhxy@cuit.edu.cn (J.L.)

* Correspondence: xch@cuit.edu.cn; Tel.: +86-28-8596-6070

Abstract: Alkali metal K- and/or Na-promoted FeCoCuAl catalysts were synthesized by precipitation and impregnation, and their physicochemical and catalytic performance for CO₂ hydrogenation to light hydrocarbons was also investigated in the present work. The results indicate that Na and/or K introduction leads to the formation of active phase metallic Fe and Fe-Co crystals in the order Na < K < K-Na. The simultaneous introduction of Na and K causes a synergistic effect on increasing the basicity and electron-rich property, promoting the formation of active sites Fe@Cu and Fe-Co@Cu with Cu⁰ as a crystal core. These effects are advantageous to H₂ dissociative adsorption and CO₂ activation, giving a high CO₂ conversion with hydrogenation. Moreover, electron-rich Fe@Cu (110) and Fe-Co@Cu (200) provide active centers for further H₂ dissociative adsorption and O-C-Fe intermediate formation after adsorption of CO produced by RWGS. It is beneficial for carbon chain growth in C₂⁺ hydrocarbons, including olefins and alkanes. FeCoCuAl simultaneously modified by K-Na exhibits the highest CO₂ conversion and C₂⁺ selectivity of 52.87 mol% and 89.70 mol%, respectively.



Citation: Zheng, Y.; Xu, C.; Zhang, X.; Wu, Q.; Liu, J. Synergistic Effect of Alkali Na and K Promoter on Fe-Co-Cu-Al Catalysts for CO₂ Hydrogenation to Light Hydrocarbons. *Catalysts* **2021**, *11*, 735. <https://doi.org/10.3390/catal11060735>

Academic Editor: Giuseppe Bonura

Received: 1 June 2021
Accepted: 10 June 2021
Published: 15 June 2021

Publisher's Note: MDPI stays neutral with regard to jurisdictional claims in published maps and institutional affiliations.



Copyright: © 2021 by the authors. Licensee MDPI, Basel, Switzerland. This article is an open access article distributed under the terms and conditions of the Creative Commons Attribution (CC BY) license (<https://creativecommons.org/licenses/by/4.0/>).

Keywords: Fe-Co@Cu alloy; CO₂ hydrogenation; dissociative adsorption; light hydrocarbons

1. Introduction

With the development of industrialization and urbanization, a large amount of CO₂ with a greenhouse effect has been discharged due to excessive use of fossil fuels, such as petroleum, coal and natural gas. The negative effects associated with increasing atmospheric concentrations of CO₂, climate change and ocean acidification, are considered as the most challenging issues of the 21st century [1,2]. Many efforts must be put forth to decrease CO₂ direct emissions, permanently sequester CO₂ and convert CO₂ to valuable products [3]. In recent years, CO₂ catalytic conversion has been a rapidly growing field because CO₂ is an abundant, non-toxic and low-cost C₁ feedstock that can be converted to many valuable chemicals and energy storage substances, such as methane [4], methanol [5–7], low-carbon alkanes [8] and olefins [9,10]. Among these, CO₂ selective hydrogenation to light hydrocarbons, including alkanes and olefins, is the most promising route [10]. For example, ethylene and propylene are the top two petrochemicals produced worldwide with a high demand for the production of plastics, polymers, solvents and cosmetics.

In the process of CO₂ hydrogenation to C₂⁺ hydrocarbons, a reverse water–gas shift reaction (RWGS) to CO over the reported Fe and Co-based catalysts is the key step, followed by a Fischer–Tropsch synthesis (FTS) reaction [11,12]. From the reported results, it has been found that FTS mainly produces light hydrocarbons over Fe-based catalysts and heavier hydrocarbons over Co-based catalysts exhibiting better chain growth potential during CO₂ hydrogenation [13–15]. Meanwhile, a Fe or Co monometallic catalyst gives a poor C₂⁺ hydrocarbon selectivity, and produces more undesired CO and CH₄ [16,17]. Therefore, Fe-Co or Fe-Cu bimetallic catalysts are adopted, and corresponding promoters are also introduced to increase catalytic activity and C₂⁺ selectivity [18–20]. This is because the bimetallic catalysts can produce metallic alloy active sites after reduction, favoring H₂

activation for RWGS. The introduced promoters mainly include transition metals such Zn, Ti and Zr [14,17,21], and alkali metals, especially K [19,22,23]. The introduced transition metals increase the electron-rich property of the catalytic active metallic phase, which is helpful for the adsorption of H₂ and CO activation followed by C-C coupling. Additionally, the alkali metal K ions can provide surface basic sites favoring CO₂ adsorption, interacting with the metallic phase and inhibiting the deep hydrogenation of carbon chains to alkanes during FTS [17,24,25]. Meanwhile, K modification is found to result in the formation of an Fe₅C₂ intermediate that enhances the RWGS reaction and then undergoes the FTS process and suppresses the secondary reaction and methane formation to obtain more hydrocarbons [23,26]. Similarly, it is also found that the presence of Na, another common alkaline metal, helps to increase CO₂ conversion and product selectivity, which contributes to the formation and stabilization of intermediate Fe_xC_y as an active species to enhance adsorption of CO₂ and weaken further hydrogenation of olefins to alkanes [27,28].

As is well known, hydroxide and carbonate of sodium are usually used as precipitants for preparing precursors of metal oxide catalysts from precipitation, in which there are often some residual sodium ions. To date, it is not clear whether the co-existence of Na and K affects CO₂ hydrogenation to light hydrocarbons over Fe- and/or Co-based catalysts. Therefore, FeCoCu-based catalysts with Al as a support component are synthesized by precipitation using Na₂CO₃-NaOH and K₂CO₃-KOH as precipitants, respectively. The obtained FeCoCuAl catalysts before and after K and/or Na modification are characterized by X-ray diffraction (XRD), N₂ adsorption-desorption, H₂ temperature-programmed reduction (H₂-TPR), CO₂ temperature-programmed desorption (CO₂-TPD), H₂ temperature-programmed desorption (H₂-TPD) and X-ray photoelectron spectroscopy (XPS). Combining catalytic tests, the effect of Na and/or K modification on the physicochemical and catalytic properties of FeCoCuAl in CO₂ hydrogenation to light hydrocarbons are investigated in the present work.

2. Results and Discussion

2.1. Textual and Structural Properties

The obtained FeCoCuAl catalyst, using sodium alkali as a precipitant, was found by ICP-OES to contain low residual Na with a Na/Fe molar ratio of 0.16%, and using potassium alkali as a precipitant gives a residual amount of K of the K/Fe molar ratio of 0.18%. From Table 1, the BET specific surface area, pore volume and average pore diameter of FeCoCuAl oxide catalysts obtained by using Na alkali solution (NaOH-Na₂CO₃) are bigger than those with K alkali solution (KOH-K₂CO₃) as a precipitant. At the same time, it is clear that Na modification can further increase the BET specific surface area, pore volume and average pore diameter of FeCoCuAl catalysts. K modification has a reverse function, which can be also proved by N₂ adsorption-desorption results of FeCoCuAl catalysts with different K and/or Na amount (see Tables S1 and S2 in Supplementary Materials). This mainly because the Na ion has a small ionic radius and easily occupies macropores to form new micropores, providing a larger surface, which can be proved by the decrease in the average pore diameter. However, the introduced K ions with a bigger ionic radius possibly block pores, especially some micropores.

Table 1. Textural properties of K- and/or Na-promoted FCCA catalysts.

Catalysts	BET Specific Surface Area (m ² ·g ⁻¹)	BJH Pore Volume (mL·g ⁻¹)	Average Pore Diameter (nm)
FCCA-N	134.1	0.42	4.1
FCCA-K	102.9	0.32	4.0
3.4Na-FCCA-K	135.9	0.34	3.2
9.3K-FCCA-N	105.4	0.36	4.2
9.3K-3.4Na-FCCA-N	110.3	0.28	3.2

From XRD results (Figure 1), the reduced FeCoCuAl catalysts synthesized by using both alkali solutions as precipitants are found to exhibit some obvious diffraction peaks at $2\theta = 18.5^\circ, 30.3^\circ, 35.8^\circ, 43.5^\circ, 54.0^\circ, 57.6^\circ, 63.1^\circ$ and 74.7° , respectively. They are assigned to characteristic diffraction peaks of Fe_3O_4 (pdf No. 65-3107) or CoFe_2O_4 (pdf No. 2-1045) [29]. Meanwhile, the weak diffraction peaks that appear at $2\theta = 43.5^\circ$ and 50.3° are characteristic of metallic Cu (pdf No. 1-1241), and the diffraction peaks assigned to metallic Fe (pdf No. 3-1050) or Fe-Co alloy (pdf No. 65-6829) are found to exhibit weak signals. This indicates that iron and cobalt oxides in catalysts are difficult to reduce to a metallic state. When promoter Na is introduced, these characteristic diffraction peaks of metallic Cu, Fe_3O_4 or CoFe_2O_4 weaken, and a new diffraction peak assigned to the (110) crystal face of metallic Fe at $2\theta = 44.5^\circ$ appears. Additionally, these changes are more obvious after K modification. Moreover, the simultaneous modification of Na and K makes characteristic diffraction peaks of Fe and Co oxides nearly disappear, and further increases the intensity of the diffraction peak at $2\theta = 44.5^\circ$, along with an obvious new peak at 65.3° assigned to the (200) crystal face of the metallic Fe-Co alloy. These show that the modification of alkali metals, Na and K ions, is helpful in the reduction of iron and cobalt species to metallic Fe or Fe-Co alloy in FeCoCuAl catalysts [30]. From XRD results, it can also be found that the reduction of copper oxide is easier than that of iron and cobalt oxides. The weakness and disappearance of metal Cu diffraction peaks after Na and/or K modification also show that copper species are reduced first. During catalyst reduction, the produced metallic Fe and Co crystals grow on the surface of metallic Cu cores. Therefore, active species of the present FeCoCuAl catalyst with K and/or Na modification are deduced to be metallic Fe or Fe-Co alloy deposited on Cu as a crystal core, which are denoted as Fe@Cu and Fe-Co@Cu, respectively. These can also be proved by XRD results of FeCoCuAl catalysts with different K and/or Na amount (see Figures S1–S3 in Supplementary Materials). The formation of Co@Cu is difficult because of a low Co content with an Fe/Co molar ratio of 3. On the other hand, no distinct diffraction signals assigned to Al-containing species are observed in the XRD pattern, indicating that Al species in reduced catalysts perhaps exist in the form of highly dispersed amorphous aluminum oxide species. Therefore, it can be concluded that the simultaneous modification of alkali metals K and Na gives rise to a synergistic effect when producing Fe@Cu and Fe-Co@Cu crystals on FeCoCuAl samples during reduction.

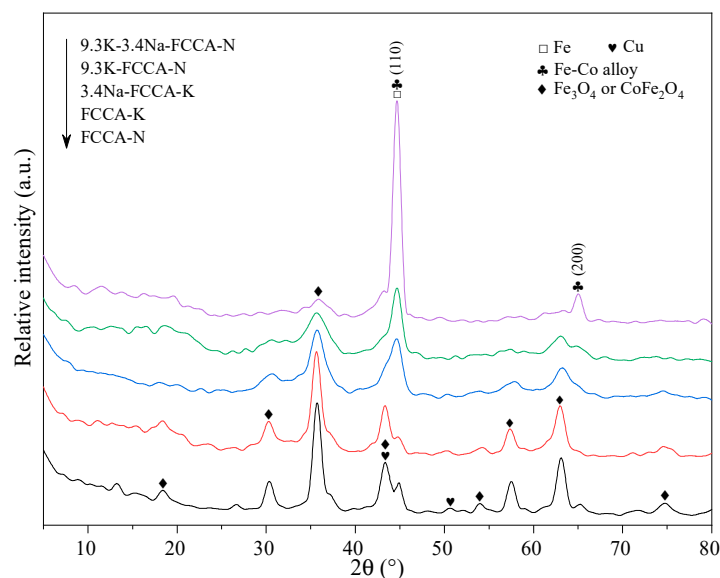


Figure 1. XRD pattern of reduced FeCoCuAl catalysts before and after K and/or Na modification. Catalyst reduction at 400°C for 1 h in pure H_2 .

2.2. H₂-TPR

As shown in H₂-TPR profiles of FeCoCuAl catalysts (Figure 2), both FCCA-N and FCCA-K exhibit a sharp reduction peak at about 256 °C, which is perhaps from H₂ consumption due to the reduction of Cu²⁺ → Cu⁰ [31], Fe³⁺ → Fe²⁺ [32] and Co³⁺ → Co²⁺ [33]. Additionally, these reduced Fe and Co species are highly dispersed due to ready occurrence of their reduction only at a low temperature. When the Na promoter is introduced into FCCA-K, this reduction peak becomes broad and slightly shifts to a high temperature. This is mainly because the presence of Na ions promotes the reduction of iron and cobalt oxides to a metallic state. Moreover, the modification of K and K-Na can further make the reduction peak broader and shift to a higher temperature. Additionally, the simultaneous introduction of K and Na brings forth a new broad reduction peak near 500 °C, which is possibly from the reduction of iron and cobalt species in CoFe₂O₄. These results indicate that Na and K modification is beneficial to the easy reduction of Fe²⁺ and Co²⁺, forming metallic Fe and Fe-Co alloy, which can be further proved by H₂-TPR profiles of FeCoCuAl catalysts with different K and/or Na amount (see Figures S4–S6 in Supplementary Materials). The improvement order is Na < K < K-Na modification. From H₂-TPR results, it can be proved that Cu⁰ crystal core should be produced first, and followed by the formation of Fe@Cu and Fe-Co@Cu crystals during reduction by H₂, in agreement with the above XRD results.

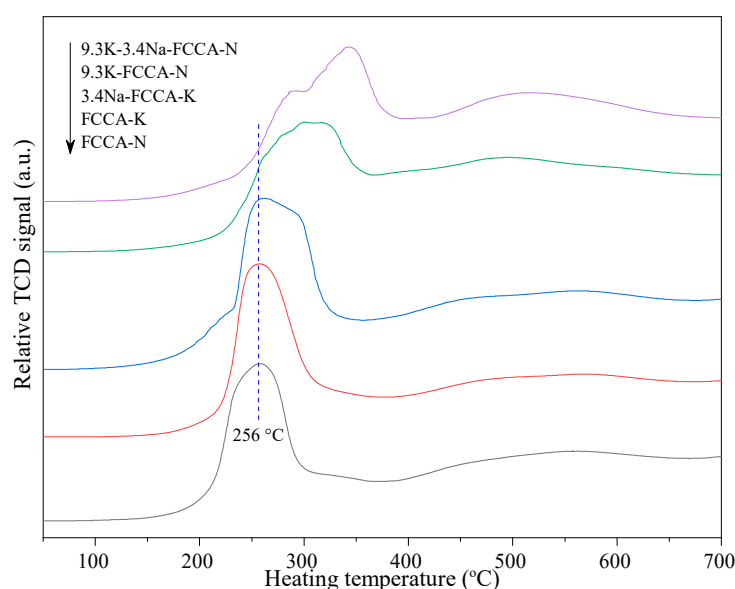


Figure 2. H₂-TPR profiles of FeCoCuAl catalysts before and after K and/or Na modification.

2.3. H₂- and CO₂-TPD

H₂-TPD curves of all reduced FeCoCuAl catalysts are shown in Figure 3. FCCA-N without K modification exhibits a broad H₂ desorption peak in a temperature range of 110–300 °C, which can be assigned to the desorption of H₂ species bonded with O atoms of iron oxide and CoFe₂O₄ species exposed on the catalyst surface [34]. However, FCCA-K without Na modification exhibits a wide H₂ desorption band in a higher temperature range of 200–470 °C. This is perhaps because FeCoCuAl synthesized by using a Na alkali solution as a precipitant contains more highly dispersed iron and cobalt oxides on the catalyst surface. When K alkali solution is used as a precipitant, the synthesized FeCoCuAl oxides are dense particles with a small surface area and pore diameter (see Table 1). This is perhaps due to the formation of Fe₃O₄-CoFe₂O₄ solid solution [29]. The ferric and cobalt oxide species in solid solution provide fewer surface O atoms. H₂ adsorption mainly occurs on the surface of metallic Cu⁰ and metallic oxide solid solution, which is difficult to reduce. Additionally, FCCA-N modified with K as a promoter exhibits a similar H₂ desorption behavior to FCCA-K. These results indicate that the obtained FeCoCuAl

catalysts, whether with K modification or using K alkali as a precipitant, contain more CoFe_2O_4 or $\text{Fe}_3\text{O}_4\text{-CoFe}_2\text{O}_4$ solid solution. Na-modified FCCA-K exhibits two obvious H_2 desorption peaks at 220°C and near 400°C , respectively. The similar results are also observed from H_2 -TPD results of FeCoCuAl catalysts with different K and/or Na amount (see Figures S7–S9 in Supplementary Materials). Additionally, these two peaks become more distinct for FCCA-N simultaneously modified by Na and K as promoters. In any case, both XRD and H_2 -TPR results have proved that Na and/or K modification leads to the easy formation of metallic Fe@Cu or Fe-Co@Cu alloy in FeCoCuAl catalysts, because alkali Na^+ and K^+ ions can provide an electron-rich environment [35]. Therefore, the obvious and broad H_2 adsorption peak bands in a temperature range of $200\text{--}420^\circ\text{C}$ are attributed to the desorption of active H formed by dissociative adsorption on metallic Fe@Cu or Fe-Co@Cu alloy species. Combined with XRD results, it can be deduced that Fe@Cu (110) or Fe-Co@Cu alloy (200) perhaps provides the main sites for H_2 dissociative adsorption.

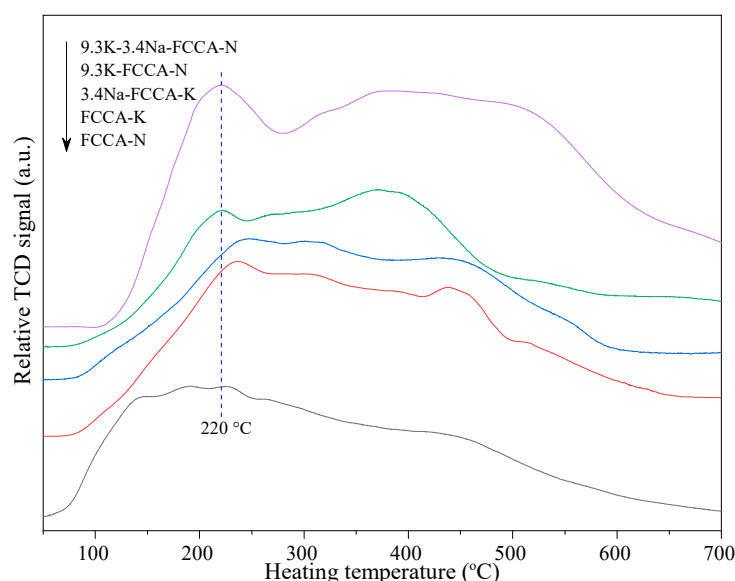


Figure 3. H_2 -TPD curves of reduced FeCoCuAl catalysts before and after K and/or Na modification. Catalyst reduction at 400°C for 1 h in pure H_2 .

CO_2 -TPD results (Figure 4) indicate that all reduced FeCoCuAl catalysts exhibit a CO_2 desorption peak at 110°C , which is attributed to weakly adsorbed CO_2 . Meanwhile, it can be observed that Na-modified FCCA-K shows a new and weak CO_2 desorption band at $350\text{--}600^\circ\text{C}$, along with a slight shift to a low temperature. This shows that the introduced sodium promoter can provide more base sites. K- and K-Na-promoted samples exhibit two obvious new CO_2 desorption peaks at about 180°C and 630°C , respectively. The similar results are also observed from CO_2 -TPD results of FeCoCuAl catalysts with different K and/or Na amount (see Figures S10–S12 in Supplementary Materials). The former is attributed to CO_2 weakly adsorbed on moderate base sites. Additionally, the latter should be from the decomposition of bidentate carbonate species produced by the strong interaction between CO_2 and potassium or sodium ferrite ($\text{K}_2\text{Fe}_2\text{O}_4$ or $\text{Na}_2\text{Fe}_2\text{O}_4$) with strong base sites [19]. This is because the alkali K^+ possesses a stronger alkalinity than Na^+ . For the same reason, the introduction of alkali metal ions can lead to the formation of electron-rich Fe@Cu and Fe-Co@Cu alloy crystals, which can also activate CO_2 molecules. All these data show that simultaneous promotion of K and Na exhibits a synergistic effect when activating H_2 and CO_2 .

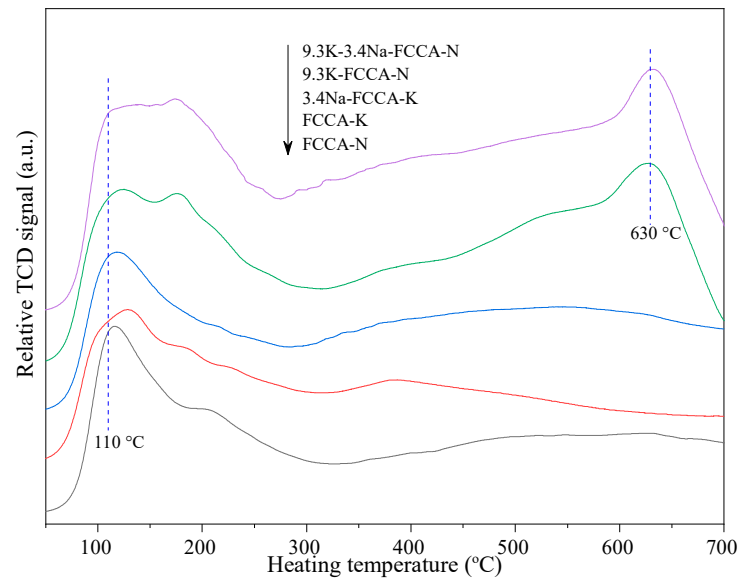


Figure 4. CO₂-TPD curves of reduced FeCoCuAl catalysts before and after K and/or Na modification. Catalyst reduction at 400 °C for 1 h in pure H₂.

2.4. XPS

From XPS results (Figure 5) of reduced samples, both FCCA-N and FCCA-K give signals at electron-binding energies of about 932.5 eV, 780.2 eV and 711.2 eV, assigned to Cu 2p_{3/2}, Co 2p_{3/2} and Fe 2p_{3/2} [18,30], respectively. Na modification gives rise to a slight decrease in all electron-binding energies of FCCA-K, and K modification leads to an obvious decrease in those of FCCA-N. The simultaneous introduction of K-Na exhibits the biggest shift to a low binding energy value. This is possibly because the introduced alkali metal ions exist in the form of oxides, which can provide more electrons for Fe@Cu or Fe-Co@Cu alloy phase [18,20]. Meanwhile, K ions have a bigger ionic radius than Na, and the corresponding oxides have a stronger capacity to provide electrons [30]. All this evidence indicates that the introduced alkali ions promote the formation of electron-rich metallic active phases in the following order: Na < K < K-Na. This shows that the simultaneous modification of alkali metals K and Na gives a synergistic effect of increasing the electron-rich property of active phase metallic Fe@Cu and Fe-Co@Cu crystals.

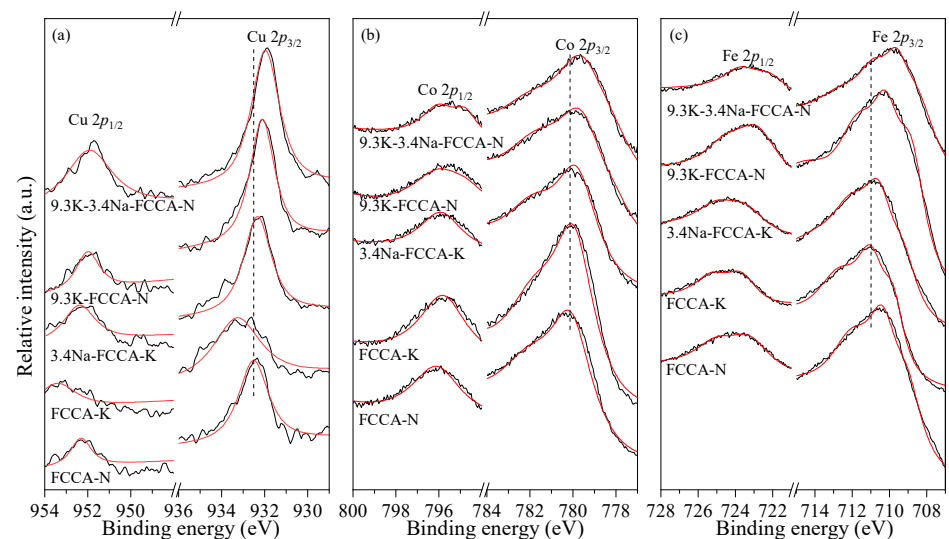


Figure 5. 2p XPS spectra of Cu (a), Co (b) and Fe (c) in reduced FeCoCuAl catalysts before and after K and/or Na modification. Catalyst reduction at 400 °C for 1 h in pure H₂.

2.5. Catalytic Performances

Catalytic activities of obtained K and/or Na-modified FeCoCuAl samples in CO₂ hydrogenation are listed in Table 2. It can be seen that a similar CO₂ conversion occurs on FeCoCuAl catalysts prepared with Na or K alkali aqueous solution as a precipitant. However, the introduction of 3.4 mol% Na, 9.3 mol% K and 3.4 mol% Na–9.3 mol% K relative to Fe leads to a sharp increase in CO₂ conversion. This is mainly because the presence of alkali K and/or Na improves the formation of Fe@Cu and Fe-Co@Cu alloy crystals and base sites, which has been proved by the XRD and CO₂-TPD results above. The formed Fe@Cu and Fe-Co@Cu alloy crystals act as catalytic active centers to activate hydrogen through dissociative adsorption. The formation of more basic sites is helpful for CO₂ adsorption and activation [36]. Additionally, the co-existence of K and Na leads to production of alkali metal ferrite, such as K₂Fe₂O₄ and Na₂Fe₂O₄, which can also activate CO₂ to form intermediate bidentate carbonate species [19]. Moreover, the presence of alkali K and/or Na ions also improves the electron-rich capacity of the (110) and (200) crystal surface of active Fe@Cu and Fe-Co@Cu, which is favorable for H₂ dissociative adsorption, proved by the H₂-TPD results above [36]. These factors accelerate CO₂ conversion to CO through a reverse water–gas shift reaction (RWGS). Meanwhile, it can be also found from Table 2 that the K promotion seems weaker than Na modification in improving CO₂ conversion, which is mainly due to the fact that the alkalinity of K ions is stronger than that of Na ions. The presence of strong base sites will promote the adsorption of more CO₂, which can occupy the space for adsorption of H₂ over the catalyst surface. Although the simultaneous introduction of 3.4 mol% Na and 9.3 mol% K can provide more strong base sites, it can also increase the formation of Fe@Cu and Fe-Co@Cu species (see XRD results) for adsorbing H₂. Therefore, it is not difficult to understand that 9.3K-3.4Na-FCCA-N exhibits the highest CO₂ conversion of 52.87 mol%.

Table 2. Catalytic properties of K- and/or Na-promoted FCCA-N in CO₂ hydrogenation.

Catalysts	CO ₂ Conversion (mol%)	Distribution of Products (mol%)				
		CO	CH ₄	C ₂ ⁺	Olefin C ₂ -C ₄	Paraffin C ₂ -C ₄
FCCA-N	35.02	2.56	26.13	71.31	20.98	44.50
FCCA-K	36.70	2.68	32.15	65.17	16.29	33.33
3.4Na-FCCA-K	47.52	4.77	10.22	85.01	28.35	40.00
9.3K-FCCA-N	46.22	2.89	17.00	80.11	25.51	33.67
9.3K-3.4Na-FCCA-N	52.87	2.29	8.01	89.70	32.14	39.98

RWGS is the first step for CO₂ hydrogenation. The produced CO can continue to react with the activated hydrogen over a catalyst. The next one is methanation to CH₄, and another is FTS reaction to C₂⁺ products including olefin and alkanes [16]. From Table 2, it is found that all catalysts give a low CO selectivity. Additionally, K modification makes FCCA-N exhibit a decreasing CH₄ selectivity and an increasing C₂⁺ hydrocarbon selectivity. Na modification also leads to a similar tendency for FCCA-K. They are also found from the catalytic property of FeCoCuAl catalysts modified by different K and/or Na amount in CO₂ hydrogenation (see Tables S1–S3 in Supplementary Materials). This is perhaps because the (110) crystal face of the formed Fe@Cu provides the active sites for dissociative adsorption of CO followed by the formation of CO-like species such as O-C-Fe@Cu and O-C-Fe-Co@Cu intermediates [24,30], which are beneficial for the carbon-chain growth for the FTS reaction to C₂⁺ hydrocarbons. At the same time, both C₂-C₄ alkanes (39.98 mol%) and CH₄ selectivity are found to decrease along with an increasing C₂-C₄ olefin selectivity (32.14 mol%) when K and Na are introduced into corresponding FeCoCuAl catalysts. This is because the introduced alkali metals ions interact with active sites in the metallic Fe and Fe-Co phase, and weaken the activity of the active hydrogen. The deep hydrogenation of CO can be inhibited to produce CH₄, and the complete hydrogenation of carbon chains to saturated hydrocarbons is prevented simultaneously. From these results, the same

conclusion as that reported in [12,19] has been drawn, that the introduced K plays a role in promoting C-C coupling and suppressing CH₄ formation during CO₂ hydrogenation. Although FCCA-N simultaneously promoted by K and Na exhibits the strongest basicity, it also has more metallic Fe@Cu and Fe-Co@Cu active sites. In particular, the increase in Fe (110) and the formation of new Fe-Co (200) crystal surfaces (see XRD results) further accelerate H₂ and CO dissociative adsorption. All these factors are advantageous for the carbon chain growth. From these catalytic data, it is found that the simultaneous modification of alkali metal K and Na provides a synergistic effect for promoting CO₂ conversion and low hydrocarbon and C₂⁺ olefin formation over FeCoCuAl catalysts during CO₂ hydrogenation.

3. Materials and Methods

3.1. Catalyst Preparation

FeCoCuAl (FCCA) catalysts were synthesized by precipitation using the corresponding nitrates as raw materials with a molar ratio of Fe³⁺:Co²⁺:Cu²⁺:Al³⁺ = 18:6:1:6. Typically, the desired amounts of Fe(NO₃)₃·9H₂O (c.p.), Co(NO₃)₂·6H₂O (c.p.), Cu(NO₃)₂·3H₂O (c.p.) and Al(NO₃)₃·9H₂O (c.p.) were dissolved in distilled water to obtain a mixture solution (total concentration of metal ions being 0.5 mol·L⁻¹). In order to ensure the modification accuracy of the introduced promoter, K or Na, two mixtures of alkali aqueous solutions including 0.6 mol·L⁻¹ NaOH-0.4 mol·L⁻¹ Na₂CO₃ and 0.6 mol·L⁻¹ KOH-0.4 mol·L⁻¹ K₂CO₃ were used as precipitants. During precipitation, the precipitant was added dropwise into the abovementioned metal ion-containing liquid mixture under stirring at room temperature until it reached pH 8.5. After finishing precipitation, precursor slurry was aged overnight, filtered and washed with distilled water until it reached pH 7.0. The obtained filter cake was dried at 110 °C, and then promoter K or Na (K₂CO₃ or NaNO₃ as raw material) was introduced to the dried FCCA catalyst precursor by impregnation, followed by calcination at 500 °C for 5 h in air atmosphere. The K-modified FCCA catalyst was denoted as 9.3K-FCCA-N with an amount of K of the K/Fe ratio of 9.3 mol%, and N as a NaOH-Na₂CO₃ mixture alkali was used as a precipitant during precursor preparation. Similarly, the Na-modified FCCA catalyst was denoted as 3.4Na-FCCA-K with a percentage of Na relative to Fe of 3.4 mol%, and the K used as a precipitant was a KOH-K₂CO₃ mixture alkali aqueous solution. The precursors of FCCA catalysts simultaneously modified by K and Na were obtained by using a NaOH-Na₂CO₃ mixture alkali as a precipitant. The modified amounts of K and Na were confirmed to be 9.3 mol% and 3.4 mol% relative to Fe, respectively, according to the optimal values reported in the literature [28,37]. This sample simultaneously modified by K and Na was denoted as 9.3K-3.4Na-FCCA-N.

3.2. Catalyst Characterization

XRD analysis of the reduced samples was carried out on a DX-2700 powder diffractometer (Dandong Fangyuan Co., China), using Cu K α radiation ($\lambda = 0.15406$ nm) with an operating condition of 40 kV, 30 mA and a scan step of 0.03°·min⁻¹.

Textural properties of all samples were measured from N₂ adsorption-desorption isotherms (−196 °C) on an SSA-4200 micromeritics instrument (Beijing Builder Co., Beijing, China). The specific surface area was calculated by the BET method according to adsorption isotherms in a relative pressure (P/P₀) range of 0.05–0.35, and pore distribution and pore diameter were calculated by the BJH method according to desorption isotherms.

H₂-TPR experiments were carried out on a PCA-1200 chemisorption analyzer equipped with a thermal conductivity detector (TCD). About 200 mg of catalysts were pretreated at 300 °C for 1 h in 30 mL·min⁻¹ N₂ flow. After cooling down to room temperature, the sample was purged with 30 mL·min⁻¹ 5% H₂-N₂ mixture gas and heated to 800 °C with a rate of 10 °C·min⁻¹. The hydrogen consumption was monitored by the TCD.

CO₂- and H₂-TPD profiles were produced on the same instrument as for H₂-TPR. For CO₂-TPD, the catalyst sample was first reduced at 400 °C for 1 h in a 5% H₂-N₂ mixture gas, followed by cooling down to 50 °C. The reduced catalyst was exposed for 30 min in

30 mL·min⁻¹ CO₂ gas flow, and then flushed with He flow for 30 min to remove physically adsorbed CO₂. After cooling to room temperature, CO₂ desorption proceeded by heating from room temperature to 800 °C in 30 mL·min⁻¹ He flow as a carrier gas, and the desorbed CO₂ amount was monitored by the TCD. For H₂-TPD, the procedure was similar to that for CO₂-TPD. The used carrier gas was Ar flow.

The chemical compositions of prepared catalysts were determined by inductively coupled plasma–optical emission spectroscopy (ICP-OES, Agilent 725 ICP). X-ray photoelectron spectroscopy (XPS) was used to analyze the chemical states of prepared catalysts on an X-ray photoelectron spectrometer system (Thermo Scientific K-Alpha, ThermoFisher, Waltham, MA, USA) equipped with a monochromated Al K α X-ray source. The binding energy (BE) was calibrated to C 1 s peak at 284.8 eV.

3.3. Catalytic Test

The catalytic performance of Na- and/or K-modified FeCoCuAl was investigated in a high-pressure fixed-bed reactor. Typically, 6 g samples (apparent volume 5.8 mL) were loaded in a stainless-steel tube reactor (internal diameter 15 mm) and reduced at 400 °C for 1 h in 50 mL·min⁻¹ pure H₂ flow under atmospheric pressure. CO₂ hydrogenation was carried out under reaction conditions of temperature 300 °C, pressure 20 atm, H₂/CO₂ ratio 3 and gas hourly space velocity (GHSV) 3000 h⁻¹. Liquid products were collected through a 0 °C cold trap connected to the reactor outlet. The distribution of H₂, CO, CH₄ and CO₂ in tail gas was found by using a gas chromatographer (GC) equipped with a TCD and TDX-01 column (1 m × 3 mm). The produced light hydrocarbons (C₁-C₅) in product gas were analyzed on-line by another GC equipped with a flame ionization detector (FID) and Kromat KB-Al₂O₃/Na₂SO₄ capillary column (30 m × 0.53 mm × 20 μ m). The collected liquid products, including water and heavy hydrocarbons, were analyzed off-line by using a GC equipped with a TCD and Paropak-Q column (4 m × 3mm). Based on the obtained GC data, CO₂ conversion and selectivity of hydrocarbons were calculated according to carbon balance. All data were obtained by averaging the values from three parallel catalytic tests.

4. Conclusions

From investigating the effect of Na and/or K modification on the physicochemical and catalytic properties of FeCoCuAl catalysts in CO₂ hydrogenation, metallic Fe@Cu and Fe-Co@Cu alloy are found to be catalytic active sites for CO₂ to CO and FTS reactions. The co-existence of Na and K in FeCoCuAl catalysts provides a synergistic effect in increasing surface basicity and the formation of Fe@Cu (110) and Fe-Co@Cu (200). Basic species provide active sites for CO₂ adsorption, which is the key step for CO₂ hydrogenation to CO through RWGS. H₂ and CO dissociative adsorption easily occur on the crystal surface of Fe@Cu (110) and Fe-Co@Cu (200), especially in the form of an electron-rich state, improved by the co-existence of K and Na. All factors accelerate carbon chain growth through C-C coupling during FTS reactions to more C₂⁺ products. K and/or Na modification is found to improve the catalytic performance of FeCoCuAl in CO₂ hydrogenation to light hydrocarbons in the following order: Na < K < K-Na. FeCoCuAl with the co-existence of K and Na exhibits the highest CO₂ conversion and C₂⁺ selectivity of 52.87 mol% and 89.70 mol%, respectively.

Supplementary Materials: The following are available online at <https://www.mdpi.com/article/10.3390/catal11060735/s1>, Figure S1: XRD pattern of the reduced FCCA-N modified with different amount of promoter K, Figure S2: XRD pattern of the reduced FCCA-K modified with different amount of promoter Na, Figure S3: XRD pattern of reduced K-Na-FCCA-N catalysts (K/Fe 9.3mol%) modified by different Na content, Figure S4: H₂-TPR profiles of FCCA-N catalysts promoted with different amount of K, Figure S5: H₂-TPR profiles of FCCA-K catalysts promoted with different amount of Na, Figure S6: H₂-TPR profiles of K-Na-FCCA-N catalysts (K/Fe 9.3mol%) promoted with different amount of Na, Figure S7: H₂-TPD profiles of FCCA-N catalysts promoted with different amount of K, Figure S8: H₂-TPD profiles of FCCA-K catalysts promoted with different

amount of Na, Figure S9: H₂-TPD profiles of K-Na-FCCA-N catalysts (K/Fe 9.3mol%) promoted with different amount of Na, Figure S10: CO₂-TPD profiles of FCCA-N catalysts promoted with different amount of K, Figure S11: CO₂-TPD profiles of FCCA-K catalysts promoted with different amount of Na, Figure S12: CO₂-TPD profiles of K-Na-FCCA-N catalysts (K/Fe 9.3mol%) promoted with different amount of Na, Table S1: Textural and catalytic properties of K-promoted FCCA-N in CO₂ hydrogenation, Table S2: Textural and catalytic properties of Na-promoted FCCA-K in CO₂ hydrogenation, Table S3: Textural property and catalytic performance of Na-promoted K-FCCA-N catalysts (K/Fe 9.3mol%) in CO₂ hydrogenation.

Author Contributions: Methodology, C.X.; investigation, X.Z.; writing—original draft preparation, Y.Z. and Q.W.; writing—review and editing, J.L.; supervision, C.X. All authors have read and agreed to the published version of the manuscript.

Funding: This research was funded by International Corporation Projects from the Department of Science and Technology of Sichuan Province (2019YFH0133) and the Sichuan Provincial Department of Education (14CZ0020).

Data Availability Statement: Data is contained within the article or supplementary material.

Acknowledgments: We would like to thank Mengdie Li from the Shiyanjia Lab for her help with XPS experiments.

Conflicts of Interest: The authors declare no conflict of interest.

References

1. Ballantyne, A.P.; Alden, C.B.; Miller, J.B.; Tans, P.P.; White, J.W.C. Increase in observed net carbon dioxide uptake by land and oceans during the past 50 years. *Nature* **2012**, *488*, 70–72. [[CrossRef](#)]
2. Wang, S.; Li, G.; Fang, C. Urbanization, economic growth, energy consumption, and CO₂ emissions: Empirical evidence from countries with different income levels. *Renew. Sustain. Energy Rev.* **2018**, *81*, 2144–2159. [[CrossRef](#)]
3. Song, C. Global challenges and strategies for control, conversion and utilization of CO₂ for sustainable development involving energy, catalysis, adsorption and chemical processing. *Catal. Today* **2006**, *115*, 2–32. [[CrossRef](#)]
4. Wang, W.; Gong, J. Methanation of carbon dioxide: An overview. *Front. Chem. Sci. Eng.* **2011**, *5*, 2–10. [[CrossRef](#)]
5. Kattel, S.; Ramírez, P.J.; Chen, J.G.; Rodriguez, J.A.; Liu, P. Active sites for CO₂ hydrogenation to methanol on Cu/ZnO catalysts. *Science* **2017**, *355*, 1296–1299. [[CrossRef](#)] [[PubMed](#)]
6. Hou, X.-X.; Xu, C.-H.; Liu, Y.-L.; Li, J.-J.; Hu, X.-D.; Liu, J.; Liu, J.-Y.; Xu, Q. Improved methanol synthesis from CO₂ hydrogenation over CuZnAlZr catalysts with precursor pre-activation by formaldehyde. *J. Catal.* **2019**, *379*, 147–153. [[CrossRef](#)]
7. Ren, H.; Xu, C.-H.; Zhao, H.-Y.; Wang, Y.-X.; Liu, J.; Liu, J.-Y. Methanol synthesis from CO₂ hydrogenation over Cu/ γ -Al₂O₃ catalysts modified by ZnO, ZrO₂ and MgO. *J. Ind. Eng. Chem.* **2015**, *28*, 261–267. [[CrossRef](#)]
8. Li, W.; Wang, H.; Jiang, X.; Zhu, J.; Liu, Z.; Guo, X.; Song, C. A short review of recent advances in CO₂ hydrogenation to hydrocarbons over heterogeneous catalysts. *RSC Adv.* **2018**, *8*, 7651–7669. [[CrossRef](#)]
9. Li, Z.; Wang, J.; Qu, Y.; Liu, H.; Tang, C.; Miao, S.; Feng, Z.; An, H.; Li, C. Highly Selective Conversion of Carbon Dioxide to Lower Olefins. *ACS Catal.* **2017**, *7*, 8544–8548. [[CrossRef](#)]
10. Guo, L.; Sun, J.; Ge, Q.; Tsubaki, N. Recent advances in direct catalytic hydrogenation of carbon dioxide to valuable C₂⁺ hydrocarbons. *J. Mater. Chem. A* **2018**, *6*, 23244–23262. [[CrossRef](#)]
11. Zhong, L.; Yu, F.; An, Y.; Zhao, Y.; Sun, Y.; Li, Z.; Lin, T.; Lin, Y.; Qi, X.; Dai, Y.; et al. Cobalt carbide nanoprisms for direct production of lower olefins from syngas. *Nature* **2016**, *538*, 84–87. [[CrossRef](#)]
12. Jiang, F.; Zhang, M.; Liu, B.; Xu, Y.; Liu, X. Insights into the influence of support and potassium or sulfur promoter on iron-based Fischer–Tropsch synthesis: Understanding the control of catalytic activity, selectivity to lower olefins, and catalyst deactivation. *Catal. Sci. Technol.* **2017**, *7*, 1245–1265. [[CrossRef](#)]
13. Yang, H.; Zhang, C.; Gao, P.; Wang, H.; Li, X.; Zhong, L.; Wei, W.; Sun, Y. A review of the catalytic hydrogenation of carbon dioxide into value-added hydrocarbons. *Catal. Sci. Technol.* **2017**, *7*, 4580–4598. [[CrossRef](#)]
14. Wang, X.; Wu, D.; Zhang, J.; Gao, X.; Ma, Q.; Fan, S.; Zhao, T.-S. Highly selective conversion of CO₂ to light olefins via Fischer–Tropsch synthesis over stable layered K–Fe–Ti catalysts. *Appl. Catal. A* **2019**, *573*, 32–40. [[CrossRef](#)]
15. Leckel, D. Diesel Production from Fischer–Tropsch: The Past, the Present, and New Concepts. *Energy Fuel.* **2009**, *23*, 2342–2358. [[CrossRef](#)]
16. Dorner, R.W.; Hardy, D.R.; Williams, F.W.; Willauer, H.D. Heterogeneous catalytic CO₂ conversion to value-added hydrocarbons. *Energy Environ. Sci.* **2010**, *3*, 884–890. [[CrossRef](#)]
17. Zhang, J.; Su, X.; Wang, X.; Ma, Q.; Fan, S.; Zhao, T.-S. Promotion effects of Ce added Fe–Zr–K on CO₂ hydrogenation to light olefins. *React. Kinet. Mech. Catal.* **2018**, *124*, 575–585. [[CrossRef](#)]
18. Wang, W.; Jiang, X.; Wang, X.; Song, C. Fe–Cu Bimetallic Catalysts for Selective CO₂ Hydrogenation to Olefin-Rich C₂⁺ Hydrocarbons. *Ind. Eng. Chem. Res.* **2018**, *57*, 4535–4542. [[CrossRef](#)]

19. Sathawong, R.; Koizumi, N.; Song, C.; Prasassarakich, P. Light olefin synthesis from CO₂ hydrogenation over K-promoted Fe–Co bimetallic catalysts. *Catal. Today* **2015**, *251*, 34–40. [[CrossRef](#)]
20. Gnanamani, M.K.; Hamdeh, H.H.; Jacobs, G.; Shafer, W.D.; Hopps, S.D.; Thomas, G.A.; Davis, B.H. Hydrogenation of Carbon Dioxide over K-Promoted FeCo Bimetallic Catalysts Prepared from Mixed Metal Oxalates. *ChemCatChem* **2017**, *9*, 1303–1312. [[CrossRef](#)]
21. Zhang, J.; Lu, S.; Su, X.; Fan, S.; Ma, Q.; Zhao, T. Selective formation of light olefins from CO₂ hydrogenation over Fe–Zn–K catalysts. *J. CO₂ Util.* **2015**, *12*, 95–100. [[CrossRef](#)]
22. Visconti, C.G.; Martinelli, M.; Falbo, L.; Infantes-Molina, A.; Lietti, L.; Forzatti, P.; Iaquaniello, G.; Palo, E.; Picutti, B.; Brignoli, F. CO₂ hydrogenation to lower olefins on a high surface area K-promoted bulk Fe-catalyst. *Appl. Catal. B* **2017**, *200*, 530–542. [[CrossRef](#)]
23. Fischer, N.; Henkel, R.; Hettel, B.; Iglesias, M.; Schaub, G.; Claeys, M. Hydrocarbons via CO₂ Hydrogenation Over Iron Catalysts: The Effect of Potassium on Structure and Performance. *Catal. Lett.* **2015**, *146*, 509–517. [[CrossRef](#)]
24. Amoyal, M.; Vidruk-Nehemya, R.; Landau, M.V.; Herskowitz, M. Effect of potassium on the active phases of Fe catalysts for carbon dioxide conversion to liquid fuels through hydrogenation. *J. Catal.* **2017**, *348*, 29–39. [[CrossRef](#)]
25. Numpilai, T.; Chanlek, N.; Poo-Arporn, Y.; Cheng, C.K.; Siri-Nguan, N.; Sornchamni, T.; Chareonpanich, M.; Kongkachuichay, P.; Yigit, N.; Rupprechter, G.; et al. Tuning Interactions of Surface-adsorbed Species over Fe–Co/K–Al₂O₃ Catalyst by Different K Contents: Selective CO₂ Hydrogenation to Light Olefins. *ChemCatChem* **2020**, *12*, 3306–3320. [[CrossRef](#)]
26. Cheng, J.; Hu, P.; Ellis, P.; French, S.; Kelly, G.; Lok, C.M. Density Functional Theory Study of Iron and Cobalt Carbides for Fischer–Tropsch Synthesis. *J. Phys. Chem. C* **2010**, *114*, 1085–1093. [[CrossRef](#)]
27. Liang, B.; Duan, H.; Sun, T.; Ma, J.; Liu, X.; Xu, J.; Su, X.; Huang, Y.; Zhang, T. Effect of Na Promoter on Fe-Based Catalyst for CO₂ Hydrogenation to Alkenes. *ACS Sustain. Chem. Eng.* **2019**, *7*, 925–932. [[CrossRef](#)]
28. Wei, J.; Sun, J.; Wen, Z.; Fang, C.; Ge, Q.; Xu, H. New insights into the effect of sodium on Fe₃O₄- based nanocatalysts for CO₂ hydrogenation to light olefins. *Catal. Sci. Technol.* **2016**, *6*, 4786–4793. [[CrossRef](#)]
29. Gnanamani, M.K.; Jacobs, G.; Hamdeh, H.H.; Shafer, W.D.; Liu, F.; Hopps, S.D.; Thomas, G.A.; Davis, B.H. Hydrogenation of Carbon Dioxide over Co–Fe Bimetallic Catalysts. *ACS Catal.* **2016**, *6*, 913–927. [[CrossRef](#)]
30. Hwang, S.-M.; Han, S.J.; Min, J.E.; Park, H.-G.; Jun, K.-W.; Kim, S.K. Mechanistic insights into Cu and K promoted Fe-catalyzed production of liquid hydrocarbons via CO₂ hydrogenation. *J. CO₂ Util.* **2019**, *34*, 522–532. [[CrossRef](#)]
31. Wan, H.; Wu, B.; Zhang, C.; Xiang, H.; Li, Y. Promotional effects of Cu and K on precipitated iron-based catalysts for Fischer–Tropsch synthesis. *J. Mol. Catal. A* **2008**, *283*, 33–42. [[CrossRef](#)]
32. Cheng, K.; Virginie, M.; Ordonsky, V.V.; Cordier, C.; Chernavskii, P.A.; Ivantsov, M.I.; Paul, S.; Wang, Y.; Khodakov, A.Y. Pore size effects in high-temperature Fischer–Tropsch synthesis over supported iron catalysts. *J. Catal.* **2015**, *328*, 139–150. [[CrossRef](#)]
33. Hou, Z.; Yashima, T. Supported Co catalysts for methane reforming with CO. *React. Kinet. Catal. Lett.* **2004**, *81*, 153–159. [[CrossRef](#)]
34. Liu, B.; Geng, S.; Zheng, J.; Jia, X.; Jiang, F.; Liu, X. Unravelling the New Roles of Na and Mn Promoter in CO₂ Hydrogenation over Fe₃O₄ -Based Catalysts for Enhanced Selectivity to Light α -Olefins. *ChemCatChem* **2018**, *10*, 4718–4732. [[CrossRef](#)]
35. Liu, J.; Zhang, A.; Jiang, X.; Liu, M.; Sun, Y.; Song, C.; Guo, X. Selective CO₂ Hydrogenation to Hydrocarbons on Cu-Promoted Fe-Based Catalysts: Dependence on Cu–Fe Interaction. *ACS Sustain. Chem. Eng.* **2018**, *6*, 10182–10190. [[CrossRef](#)]
36. Wang, X.; Zhang, J.; Chen, J.; Ma, Q.; Fan, S.; Zhao, T.-S. Effect of preparation methods on the structure and catalytic performance of Fe–Zn/K catalysts for CO₂ hydrogenation to light olefins. *Chin. J. Chem. Eng.* **2018**, *26*, 761–767. [[CrossRef](#)]
37. Prasad, P.S.S.; Bae, J.W.; Jun, K.-W.; Lee, K.-W. Fischer–Tropsch Synthesis by Carbon Dioxide Hydrogenation on Fe-Based Catalysts. *Catal. Surv. Asia* **2008**, *12*, 170–183. [[CrossRef](#)]